Dissymmetric Triaryltriazines: Small Mass Columnar Glasses

Fabrícia Nunes da Silva, Hugo Marchi Luciano, Carlos Stadtlober, Giliandro Farias, Fabien Durola, Juliana Eccher, Ivan Bechtold, Harald Bock, Hugo Gallardo, André Vieira

Dissymmetric Triaryltriazines: Small Mass Columnar Glasses

Fabrícia Nunes da Silva,[a, b] Hugo Marchi Luciano,[b, c] Carlos H. Stadtlober,[d] Giliandro Farias,[c] Fabien Durola,[e] Juliana Eccher,[d] Ivan H. Bechtold,*[d] Harald Bock,*[e] Hugo Gallardo,[c] and André A. Vieira*[a]

Abstract: Columnar liquid crystals with very small molecular masses that form anisotropic glasses well above room temperature are obtained by mixed dissymmetric substitution of *sym*-triazine with ester-bearing phenyl and phenanthryl or tetrahelicenyl moieties. The combination of low molecular symmetry with configurational flexibility and short polar ester moieties stabilizes the mesophase over large temperature ranges and induces pronounced calorimetric glass transitions within the anisotropic fluid despite the smallness of the molecules. In contrast to more symmetrical homologs, no ester tails longer than ethyl are necessary to induce the liquid crystalline state, allowing for the near-absence of any insulating and weight-increasing alkyl periphery. Films drop-cast from solution show in all cases emission spectra that do not show significant change of fluorescence emission upon annealing, indicating that the columnar hexagonal mesoscopic order is obtained directly upon deposition from solution and is resistant to crystallization upon annealing.

Introduction

Anisotropic, that is, liquid crystalline (LC), polycyclic aromatic glasses allow in principle the embedding of oriented emitter molecules in organic LEDs, to give anisotropic emission and improved light outcoupling.[1–3] Columnar LC glasses are of particular interest due to their easy homeotropic alignment and their good charge and exciton transport properties along the columnar stacks.[4–9] The design of molecular glass formers relies to a considerable extent on symmetry breaking combined with configurational flexibility, which is illustrated by the seminal case of the 1,3,5-trinaphthylbenzenes, of which the dissymmetric α,α,β-isomer has evolved into a standard-bearer for polyaromatic glass-formers.[10] Although the glass transition temperature T_g generally correlates strongly with molecular weight, the addition of flexible side chains leads to a decrease of T_g.[11] Such side chains are a key ingredient to columnar liquid crystals, but several low-symmetry arenes have been reported to form columnar mesophases in the absence of elongated side chains, examples being polychlorinated indene derivatives[12] and 1,2,3,4-tetrafluoro-6,7,10,11-tetramethoxy-triphenylene.[13]

Uniform alignment of columnar LC glasses has been achieved by controlled physical vapor deposition (PVD), and the entropy content of the glass state can be modulated by the deposition conditions.[14–16] The smaller the molecular weight, the easier the device construction by PVD. But the smaller the molecular weight, the more difficult it is to obtain a glass transition temperature T_g conveniently above room temperature. Molecular flexibility and configurational multiplicity combined with viscosity-augmenting polar substituents are ingredients that have allowed us recently to obtain columnar LC glasses with above-room-temperature T_g from extended triaryltriazine hexaesters **1** and **2** bearing three phenanthyl or three tetrahelicenyl groups on the *s*-triazine core[17] (Scheme 1). Given the presence of six propyl or butyl ester groups and three extended aryl arms, the molecular weights of these columnar glass formers are considerable (1126 and 1361 Da), and whilst **1** shows no attainable LC-to-isotropic transition (i.e. clearing point) up to 375 °C that would also allow its uniform alignment by cooling from the isotropic liquid, **2** shows only a monotropic mesophase (observable only on cooling, the melting point being higher than the clearing point). Homologs of **1** and **2** with longer alkyl ester chains do not show a T_g above room temperature, and the homologs with short ethyl chains are not LC. In contrast, the meta-configured triphenyl-triazine-triethyl ester **3** shows a viscous monotropic nematic LC phase, but no calorimetric glass transition and crystallizes over several days at room temperature.

[a] *F. Nunes da Silva, Prof. A. A. Vieira*
Instituto de Química
Universidade Federal da Bahia
Ondina, 40170-115 Salvador, BA (Brazil)
E-mail: vieira.andre@ufba.br

[b] *F. Nunes da Silva, H. Marchi Luciano*
Centre de Recherche Paul Pascal
Univ. Bordeaux
115 av. Schweitzer, 33600 Pessac (France)

[c] *H. Marchi Luciano, Dr. G. Farias, Prof. H. Gallardo*
Departamento de Química
Universidade Federal de Santa Catarina
Trindade, 88040-900 Florianópolis, SC (Brazil)

[d] *C. H. Stadtlober, Prof. J. Eccher, Prof. I. H. Bechtold*
Departamento de Física
Universidade Federal de Santa Catarina
Trindade, 88040-900 Florianópolis, SC (Brazil)
E-mail: ivan.bechtold@ufsc.br

[e] *Dr. F. Durola, Dr. H. Bock*
Centre de Recherche Paul Pascal, CNRS
115 av. Schweitzer, 33600 Pessac (France)
E-mail: harald.bock@crpp.cnrs.fr

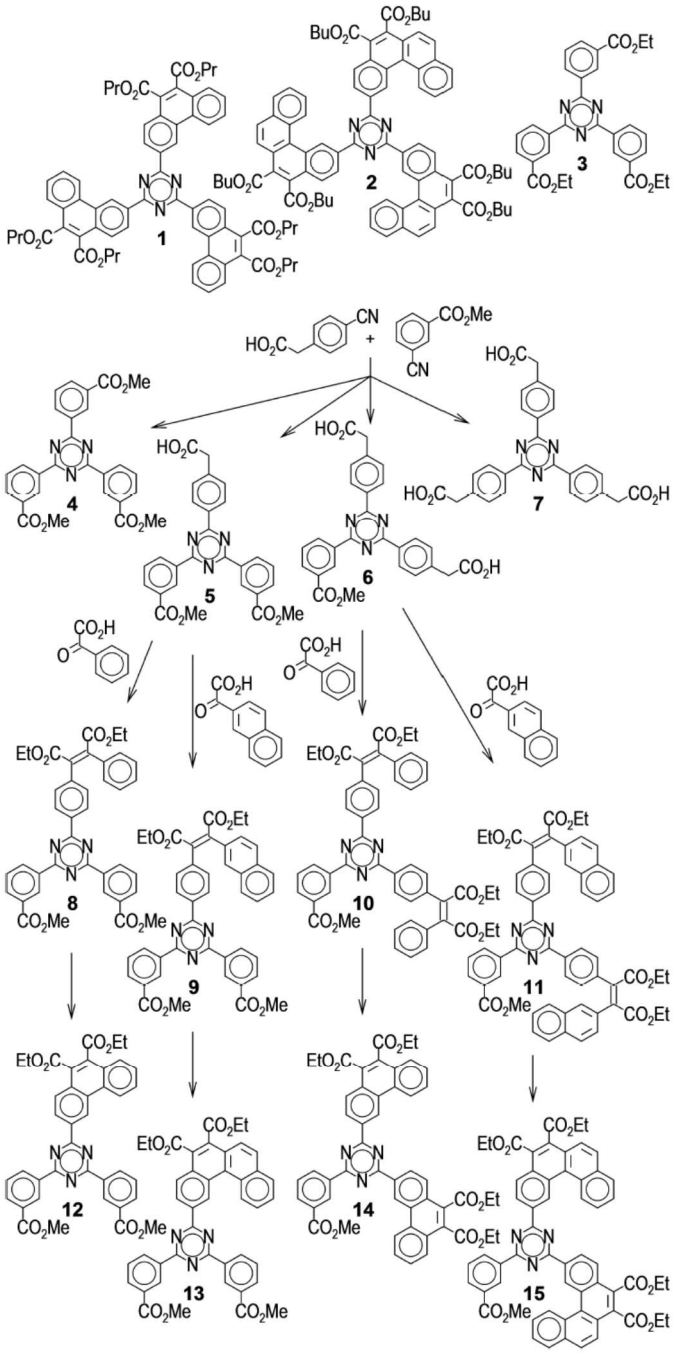

Scheme 1. Symmetric and dissymmetric mesogenic triaryltriazine esters and their precursors.

Here we report that enantiotropic columnar mesophases with attainable clearing temperatures and prominent calorimetric glass transitions above room temperature, as well as with molecular masses well below 1000 Da and attainable melting and clearing points, are obtained when the structural elements of **3** and either **1** or **2** are mixed. This hybridization of fragments is achieved via the statistical co-trimerization of methyl 3-cyanobenzoate with 4-cyanophenylacetic acid, which allows, due to the distinct polarities of the methyl ester group of the former and the free acid group of the latter, the straightforward separation of the 2:1 and 1:2 cotrimerization products.

Results and Discussion

We have earlier reported that methyl 3-cyanobenzoate is trimerized in triflic acid at room temperature without substantial hydrolysis and degradation to non-mesogenic **4**, whereas **3** itself and its longer-chain homologs are better obtained by saponification of the methyl homolog **4** followed by appropriate re-esterification than by the hydrolysis-plagued trimerization of the appropriate alkyl 3-cyanobenzoate.[18] We also noted previously that degradation upon attempted trimerization in triflic acid is a problem with 3-cyanobenzoic acid, but not with 3-cyanophenylacetic acid.[17] Accordingly, we now found that the co-trimerization of the latter with methyl 3-cyanobenzoate affords a mixture of products **4**–**7** from which **5** and **6** can be isolated conveniently by column chromatography in about 30% of the statistically expected yield.

Perkin condensation of **5** or **6** with phenylglyoxylic or 2-naphthylglyoxylic acid ($PhCOCO_2H$ or β-$C_{10}H_7COCO_2H$) followed by in situ esterification with ethanol and bromoethane to the photoreacive intermediates **8**–**11** and subsequent Mallory photocyclization led to the four target compounds **12**–**15** (Scheme 1). Not only are their molecular weights of 670, 720, 856 and 956 Da markedly lower than those of **1** and **2**, but we could also establish that, in spite of only very short methyl and ethyl ester substituents, their columnar mesophases persist at room temperature below conveniently attainable melting and clearing temperatures (Table 1 and Figure 1). Whilst the mesophases of the two tetraesters **12** and **13** are monotropic (i.e., with melting points above their clearing points), those of the pentaesters **14** and **15** are enantiotropic, i.e. with higher clearing than melting points.

The hexagonal symmetry of the mesophase is evident from its growth in non-birefringent homeotropic domains upon cooling the isotropic liquid (Inset in Figure 2), because non-birefringent homeotropic growth is not compatible with the less common rectangular and oblique symmetries sometimes alternatively encountered in columnar mesogens. As expected, **12** bearing only one phenanthrene fragment shows a much lower clearing temperature T_{cl} (of 145 °C, i.e., 22 °C below its melting point T_m of 167 °C) than the larger **14** with two phenanthrene fragments (T_{cl} = 291 °C, i.e., 86 °C above its T_m of

Table 1. Calorimetric phase transition onset temperatures (°C) and enthalpies (J/g [in brackets]), and glass transition onset temperatures, on heating with 10 °C/min; Cr = crystalline phase, Col_{hex} = hexagonal columnar mesophase, Iso = isotropic liquid, T_g(Col) = glass transition temperature in the mesophase; monotropic transitions (observed on second heating only, after cooling from the isotropic liquid) in italics. The three right-hand columns give the column-to-column distance d_{col} and the intracolumnar disk stacking distance d_{disk} in Å at 25 °C in the mesophase as observed by XRD, and the molecular mass in Da. Data for **1** and **2** are taken from the literature.[17]

	Cr-Cr	Cr-Col_{hex}	Col_{hex}-Iso	Cr-Iso	T_g(Col)	d_{col}	d_{disk}	m
12			*145*[2.8]	167[39]	*38*	16.9	3.4	670
13			*144*[3.7]	210[85]	*44*	16.9	3.4	720
14		205[41]	291[5.9]		*50*	19.0	3.3	856
15	160[21]	214[2.7]	227[4.8]		*67*	19.4	3.5	956
1		150[13]	> 375		*81*	20.8	-	1126
2			*149*[1.0]	205[34]	*39*	22.5	3.7	1361

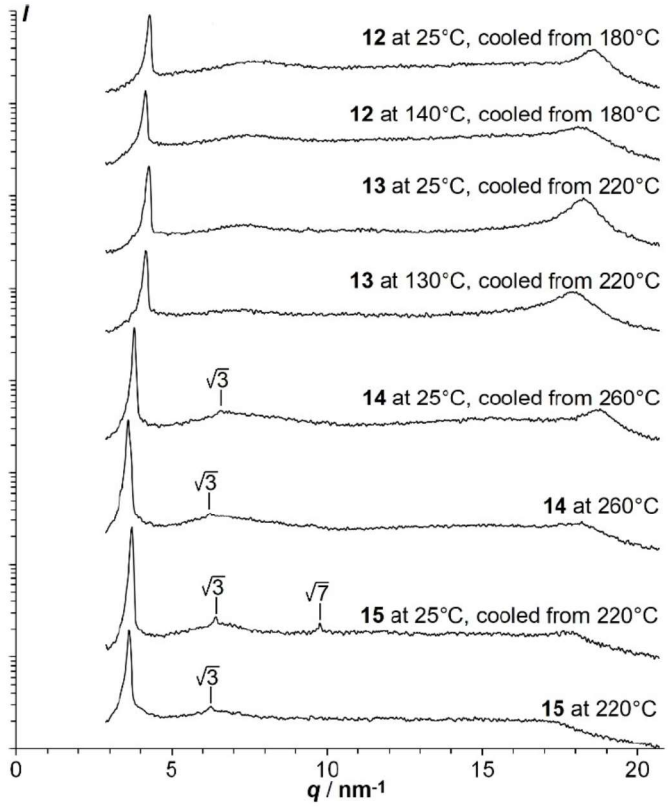

Figure 1. XRD spectra of **12**–**15** at room and elevated temperature in the columnar mesophase (logarithmic intensity scaling). The root values indicate the *q* ratio with the main lattice peak to the left and correspond to a column lattice of hexagonal symmetry.

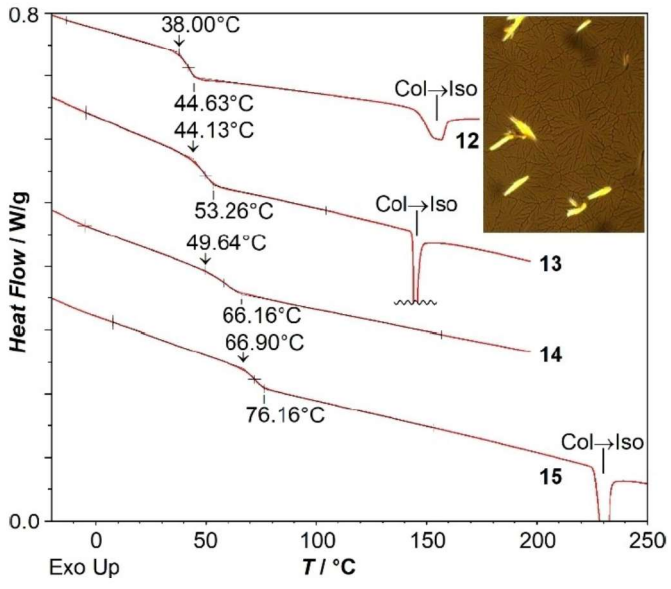

Figure 2. Differential calorimetry heating scans (red) of **12**–**15** at + 10 °C/min (after initial heating above the melting point and subsequent cooling at −10 °C/min); glass transition onset temperatures on heating are indicated above vertical arrows; phase transitions are marked between Col = hexagonal columnar mesophase and Iso = isotropic liquid. Inset: Homeotropic optical texture of **12** upon cooling from the isotropic liquid (polarizing light microscopy, slightly uncrossed polarizers).

205 °C), but both compare favorably with **1**, which does not clear within our experimental limits (< 375 °C) [all clearing and melting temperatures given are calorimetric onset temperatures on heating at 10 °C/min]. In both cases, a mesomorphic columnar glass is obtained when cooling from above T_{cl} and T_m. Glass transition temperatures T_g, taken, according to common standard, as the onset of the calorimetric heat capacity step on heating with 10 K/min, are 38 °C for **12** and 50 °C for **14** (Figure 2). The corresponding larger tetra- and penta-esters **13** and **15** with one or two tetrahelicene units and ethyl and methyl termini also show moderate T_{cl} of 144 °C (76 °C below **13's** T_m of 210 °C) and 227 °C (13 °C above **15's** T_m of 214 °C), under the effect of the planarity-disrupting helical fragments. In contrast to the conveniently lowered T_{cl} of **15** compared to **14**, **13** and **15** exhibit increased T_g of 44 °C and 67 °C, i.e., 6 and 17 °C higher than their phenanthrene homologs **12** and **14**.

Compared with monotropic **2**, the only symmetrical homolog that exhibits an attainable isotropic phase (T_{cl} = 149 °C, T_m = 205 °C, T_g = 39 °C)[17] and a columnar glass at room temperature (at the expense of a much larger molecular weight), **12**–**15** all show an improved T_g, and it is striking that **15** with two large, slightly non-planar tetrahelicenyl fragments exhibits a thermodynamically stable mesophase with an enantiotropic temperature range, whilst its more disk-shaped, but symmetrical, homolog **2** with three [4[helicenyl arms does not. In contrast, in the more planar phenanthrene homologs, the enantiotropic mesophase range is greatly reduced when going from symmetrical **1** to the bis-phenanthryl homolog **14**: whilst T_{cl} becomes attainable (> 375 °C→291 °C), T_m increases (150 °C→205 °C), and T_g decreases (81 °C→50 °C).

To confirm the hexagonal symmetry of the columnar mesophase, we recorded X-ray diffraction (XRD) spectra of **12**–**15** at room and elevated temperatures. Whereas the broad disk-to-disk stacking peak of the two phenanthryl homologs **12** and **14** testifies of a rather close stacking distance of 3.3 Å at room temperature, the less planar tetrahelicenyl groups in **13** and **15** lead to a slightly wider stacking of *ca.* 3.5 Å. The hexagonal nature of mesophase of the two derivatives **14** and **15** with two extended aryl arms is evident from the presence of the (11) secondary lattice peak corresponding to a q ratio of $\sqrt{3}$ to the main (10) lattice peak. In **15** at room temperature, the (21) peak (q ratio of $\sqrt{7}$ to main peak) is also discernible. In contrast to **14** and **15**, the one-armed derivatives **12** and **13** show no secondary lattice peaks besides the main lattice peak and the disk-to-disk stacking peak, which means that the column lattice has no well-expressed long-range periodicity. The mesophase may nevertheless be considered to be of hexagonal symmetry, because rectangular or oblique symmetry would imply splitting of the main peak, and because dense 2D packing of circular objects (such as the columns observed here) is a priori hexagonal, at least at short range.

Curiously, the disk-to-disk peak is relatively more intense in **12** and **13** than in **14** and **15**, i.e., the more pronounced the intracolumnar stacking, the less pronounced the symmetry of the column lattice. This suggests that precise stacking of low-symmetry mesogens is not well compatible with a very

symmetrical column shape, whereas looser stacking averages out more easily any column dissymmetries.

The similarity between the mesophase structures of the phenanthryl homologs **12** and **14**, as well as between the tetrahelicenyl homologs **13** and **15**, is apparent in their emission spectra from solution-cast film before and after annealing (Figure 3 and Table 2): Not only are the emission spectra of each pair in solution fully superimposable, even in condensed films nearly no difference in the emission spectra between **12** and **14** or between **13** and **15** before and after annealing can be noted. The near-identity of the emission spectra of a given material before and after annealing suggests that deposition from solution directly leads to the formation of a mesomorphic columnar glass at room temperature, without need to induce this state by annealing at higher temperatures. This hypothesis is confirmed in the XRD spectra of the non-annealed solution-cast films: For all four compounds, only a single diffraction peak corresponding to the distance between adjacent rows of columns in a high-symmetry, i.e. hexagonal, lattice is detected (see Supporting Information), with higher order peaks not observable due to the lower resolution of the spectra from the thin solution-cast films compared to those of the bulk samples (as in Figure 1), and with the disk-to-disk peak not observed due presumably to a small correlation length inside the columns in non-annealed thin film samples.

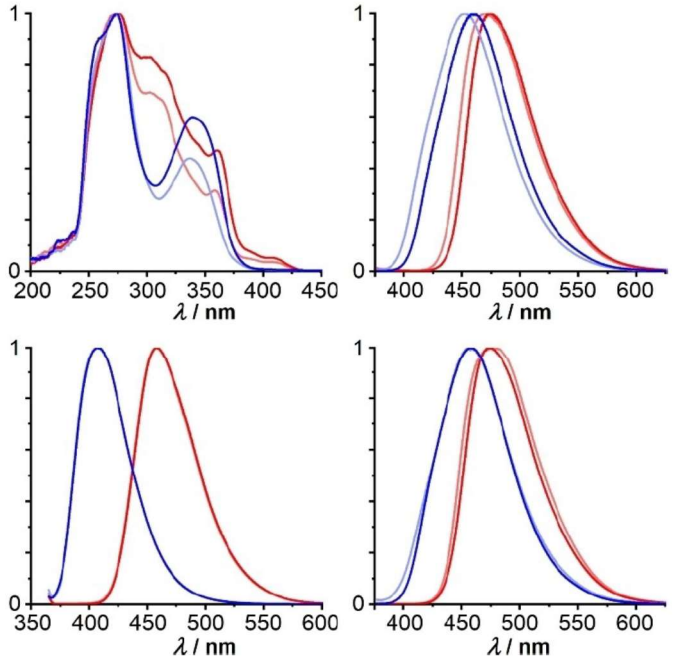

Figure 3. Left: Normalized absorption (top) and emission (bottom) in dilute chloroform solution [10^{-2} mg/mL]. Right: Normalized emission in drop-cast film at room temperature before (top) and after (bottom) heating above the melting point. Emission spectra were obtained upon excitation at 360 nm. **12**: light blue, **13**: pink, **14**: dark blue, **15**: red.

Table 2. Photoluminescence quantum yield and emission maximum in chloroform solution and in drop-cast film, upon excitation at 360 nm.

	12	13	14	15
Solution ($CHCl_3$)	30% 408 nm	23% 457 nm	37% 407 nm	17% 459 nm
As-cast film	28% 453 nm	24% 470 nm	31% 459 nm	21% 474 nm
Annealed film	21% 457 nm	22% 477 nm	35% 458 nm	19% 474 nm

The photoluminescence quantum yields in condensed film (Table 2), before or after annealing, are similar to those in solution, indicating neither pronounced enhancement nor quenching of emission by aggregation in the columnar mesomorphic solid.

The longer-wavelength parts of the absorption spectra in solution show a relative increase of absorption from **12** to **14** as well as from **13** to **15**, suggesting that the phenanthrene and tetrahelicene arms (whose number increases from **12**/**13** to **14**/**15**) are responsible for the longer-wavelength absorption maxima (**12**: 338 nm, **13**: 303 & 358 nm, **14**: 340 nm, **15**: 304 & 360 nm), whereas the intense peak at shorter wavelength common to all four compounds (**12**: 273 nm, **13**: 277 nm, **14**: 273 nm, **15**: 275 nm) may be associated with the triazine core.

To confirm the UV-Vis attributions, the excited state configurations were investigated using TD-DFT calculations on the optimized ground state geometries obtained from DFT within the B3LYP/def2-TVZP(–f) level of theory. For **12** and **14**, the low energy band is related to π-π* transitions mostly centered at phenanthrene moiety, while the high energy band is a π-π* but mostly spread through the triazine core. The two main differences in the absorption profiles of **13** and **15** can be related to the adopted geometry with lower planarity in the tetrahelicenyl moiety. The low-intensity band of these two compounds close to 425 nm arises from a charge transfer from tetrahelicenyl to triazine. Besides the π-π* triazine band at high energy, transitions spread through the tetrahelicenyl moieties are observed. The loss of planarity leads to transitions of intermediate energy in **13** and **15**, not observed in planar **12** and **14**. From **12** to **14** and from **13** to **15**, the number of excited states with similar energies increases due to the presence of two phenanthrene or two tetrahelicenyl moieties (see Supporting Information). This concords with the higher experimentally observed intensity of the lower-energy bands of **14** and **15**, as the combined transitions of similar energy sum up to the observed absorption band.

The first excited singlet state (S_1) energy obtained from the onset of emission in solution was compared to those obtained from TD-DFT for **12** (experimental/theoretical: 3.22/3.489 eV), **13** (2.92/3.059), **14** (3.07/3.361) and **15** (2.85/2.994), showing a good correspondence. Due to this good correspondence, we also calculated the energy of the excited triplet states T_1 on the same geometries using SOC-TD-DFT, obtaining 2.677 (**12**), 2.487 (**13**), 2.644 (**14**) and 2.482 (**15**) eV. This evidences that the increase in number of phenanthrene or tetrahelicenyl moieties decreases the energy of the S_1 state, while the effect on the T_1 state is negligible. Considering their T_1 energy values together with their low molecular weight, the glass-forming mesogens **12** to **15** may be considered as conveniently vapor-depositable anisotropic matrices for TADF emitters that emit green-to-yellow light of slightly lower energy than these T_1 levels.

Conclusions

The cotrimerization of differently functionalized benzonitriles allows access to small weight glass-forming columnar mesogenic triaryltriazine tetra- and pentaesters with moderate transition temperatures to the isotropic liquid. Their luminescence is not significantly reduced in condensed solid films compared to the emission of the non-aggregated molecules in dilute solution.

Thus the dissymmetrization of threefold-symmetric flexible molecular structures proves to be an efficient means to allow the formation of the mesomorphic columnar state at room temperature even in the near-absence of an alkyl periphery. This absence of fluidity-enhancing alkyl moieties allows vitrification at above-ambient temperatures even at very small **molecular** weight, yielding anisotropic luminescent glasses with accessible clearing temperatures, with potential for physical vapor deposition of alignable anisotropic emitter layers in organic electronic devices.

Experimental Section

4′,4′′-Bis(methoxycarbonyl)-2,4,6-triphenyl-*s*-triazine-4′′′-acetic acid 5 and 4′-methoxycarbonyl-2,4,6-triphenyl-*s*-triazine-4,′′4′′′-diacetic acid 6: Under ice bath cooling, triflic acid (10 mL) is added to an intimate mixture of 4-cyanoacetic acid (2.00 g, 160.2 g/mol, 12.5 mmol) and methyl 3-cyanobenzoate (2.00 g, 160.2 g/mol, 12.5 mmol), and the mixture is stirred under exclusion of moisture for 16 h at room temperature. The ensuing viscous yellow-orange solution is poured into a stirred ice-water mixture and stirred for 2 h. The white precipitate is filtered off, washed with water and air-dried. The product mixture is separated by column chromatography on silica: The unwanted triester **4** is eluted with pure chloroform, the diester-monoacid **5** is eluted thereafter with chloroform containing 5% of acetone, and finally the monoester-diacid **6** is eluted with chloroform containing 10% of acetone, leaving the unwanted triacid **7** on the column. The two separated cotrimerization products are used in the next step without further purification. Yields for **5** and **6** varied from batch to batch between 0.3 g and 0.6 g for either of them, with an average yield of 0.45 g each. The statistically expected yield presuming ideal mixing of the two starting materials leading to a 1:3:3:1 ratio between products **4**, **5**, **6** and **7** is 1.5 g of both 5 and 6, thus the average isolated yields of each the two co-trimerization products correspond to 30% of the theoretical value. Monoacid-diester 5: 1HNMR (400 MHz, DMSO-d_6): $\delta = 8.79$ (s, 2H), 8.54 (d, 2H, 8 Hz), 8.29 (d, 2H, 8 Hz), 8.03(d, 2H, 8 Hz), 7.56 (t, 2H, 8 Hz), 7.40 (d, 2H, 8 Hz), 3.89 (s, 6H), 3.66 (s, 2H) ppm. Diacid-monoester 6: 1HNMR (400 MHz, DMSO-d_6): $\delta = 9.02$ (s, 1H), 8.78 (d, 1H, 8 Hz), 8.51 (d, 4H, 8 Hz), 8.13(d, 1H, 8 Hz), 7.68 (t, 1H, 8 Hz), 7.49 (d, 4H, 8 Hz), 3.91 (s, 3H), 3.72 (s, 4H) ppm.

General procedure for the condensation of 5 or 6 with arylglyoxylic acids to 12–15: Triazine-mono- or -diacetic acid **5** or **6** (2 mmol, 480.5 g/mol each, 0.96 g) and a twofold excess (i.e. 4 or 8 mmol) of phenylglyoxylic acid or 2-naphthylglyoxylic acid are stirred at reflux in a mixture of acetic anhydride (40 mmol, 102.1 g/mol, 4.1 g), triethylamine (30 mmol, 101.2 g/mol, 3.0 g) and dry THF (60 mL) for 24 h under argon. Then the reaction is cooled to room temperature, a mixture of alkyl alcohol (240 mmol), bromoalkane (180 mmol) and triethylamine (120 mmol, 12 g) and dry THF (30 mL) is added and stirring at reflux is continued for another 24 h. Then the mixture is cooled to room temperature, poured into a stirred 1:1:1 mixture (300 mL) of ice, water and concentrated aqueous hydrochloric acid and extracted with ethyl acetate. The ethyl acetate extract is dried over magnesium sulphate and concentrated, and the residue is dissolved in a minimum amount of ethyl acetate and crystallized by adding ethanol. The obtained precipitate is dissolved in ethyl acetate (1 L), iodine (0.3 g) is added, and the solution is irradiated for 48 h at room temperature under air in a Peschl photoreactor with irradiation from a medium-pressure 150 W mercury immersion lamp inside a borosilicate immersion tube in which cooling water circulates. The solvent is evaporated, and the residue is purified by column chromatography on silica eluting with chloroform containing 1% of ethanol, followed by recrystallization from chloroform/ethanol to yield the desired triaryltriazine alkylester in 20 to 45% (on average 33%) overall yield over three steps (Perkin condensation, esterification, oxidative photocyclization).

2,4-Bis(3-(methoxycarbonyl)phenyl)-6-(9,10-bis(ethoxycarbonyl)phe-nanthren-3-yl)-*s*-triazine 12: Yield: 0.27 g (669.7 g/mol, 20%). 1HNMR (400 MHz, CD_2Cl_2): $\delta = 9.72$ (s, 1H), 9.02 (s, 2H), 8.68 (d, 1H, 8 Hz), 8.65 (d, 1H, 9 Hz), 8.61 (d, 2H, 8 Hz), 8.19 (d, 1H, 9 Hz), 8.08 (d, 3H, 8 Hz), 7.77 (t, 1H, 8 Hz), 7.69 (t, 1H, 8 Hz), 7.47 (t, 2H, 8 Hz), 4.55 (q, 2H, 7 Hz), 4.54 (q, 2H, 7 Hz), 3.95 (s, 6H), 1.52 (t, 3H, 7 Hz), 1.50 (t, 3H, 7 Hz) ppm. 13CNMR (100 MHz, CD_2Cl_2): $\delta = 171.3$, 171.1, 168.1, 167.9, 166.7, 136.3, 135.2, 133.9, 133.3, 132.5, 131.7, 131.1, 131.0, 130.5, 130.2, 129.7, 129.3, 129.2, 128.4, 127.7, 127.6, 127.3, 127.2, 124.3, 123.5, 62.7, 62.6, 52.7, 14.59, 14.57 ppm. ESI-HRMS: m/z calcd for $C_{39}H_{31}N_3O_8Na$ $[M+Na]^+$: 692.20034, found 692.1992.

2,4-Bis(3-(methoxycarbonyl)phenyl)-6-(5,6-bis(ethoxycarbonyl)[4]-he-licen-2-yl)-*ss*-triazine 13: Yield: 0.36 g (719.7 g/mol, 25%). 1HNMR (400 MHz, $CDCl_3$): $\delta = 10.58$ (s, 1H), 9.41 (s, 2H), 9.25 (d, 1H, 8 Hz), 9.01 (d, 3H, 8 Hz), 8.51 (d, 1H, 8 Hz), 8.30 (d, 2H, 8 Hz), 8.10 (d, 1H, 8 Hz), 8.07 (d, 1H, 9 Hz), 8.02 (d, 1H, 9 Hz), 7.92 (t, 1H, 8 Hz), 7.79 (t, 1H, 8 Hz), 7.68 (t, 2H, 8 Hz), 4.60 (q, 2H, 7 Hz), 4.58 (q, 2H, 7 Hz), 4.02 (s, 6H), 1.53 (t, 3H, 7 Hz), 1.49 (t, 3H, 7 Hz) ppm. 13CNMR (100 MHz, CD_2Cl_2): $\delta = 172.0$, 171.5, 168.4, 167.9, 166.9, 136.7, 134.8, 134.6, 134.0, 133.6, 132.6, 131.7, 131.4, 130.8, 130.7, 130.6, 130.2, 130.0, 129.5, 129.4, 129.1, 129.0, 128.2, 127.7, 127.3, 126.9, 126.8, 123.6, 62.8, 52.8, 14.62, 14.57 ppm. ESI-HRMS: m/z calcd for $C_{43}H_{33}N_3O_8Na$ $[M+Na]^+$: 742.21599, found 742.2161.

2-(3-(Methoxycarbonyl)phenyl)-4,6-bis(9,10-bis(ethoxycarbonyl)phe-nanthren-3-yl)-*ss*-triazine 14: Yield: 0.77 g (855.9 g/mol, 45%). 1HNMR (400 MHz, CD_2Cl_2): $\delta = 9.75$ (s, 2H), 9.01 (s, 1H), 8.68 (d, 2H, 9 Hz), 8.57 (d, 1H, 8 Hz), 8.46 (d, 2H, 8 Hz), 8.21 (d, 2H, 9 Hz), 8.06 (d, 1H, 8 Hz), 7.99 (d, 2H, 8 Hz), 7.66 (t, 2H, 8 Hz), 7.62 (t, 2H, 8 Hz), 7.46 (t, 1H, 8 Hz), 4.56 (q, 4H, 7 Hz), 4.54 (q, 4H, 7 Hz), 3.93 (s, 3H), 1.52 (t, 6H, 7 Hz), 1.51 (t, 6H, 7 Hz) ppm. 13CNMR (100 MHz, CD_2Cl_2): $\delta = 171.3$, 171.1, 168.1, 167.9, 166.7, 136.3, 135.2, 133.9, 133.3, 132.5, 131.7, 131.1, 131.0, 130.5, 130.2, 129.7, 129.3, 129.2, 128.4, 127.7, 127.6, 127.3, 127.2, 124.3, 123.5, 62.7, 62.6, 52.7, 14.59, 14.57 ppm. ESI-HRMS: m/z calcd for $C_{51}H_{41}N_3O_{10}Na$ $[M+Na]^+$: 878.26842, found 878.2682.

2-(3-(Methoxycarbonyl)phenyl)-4,6-bis(9,10-bis(ethoxycarbonyl)[4]he-licen-2-yl)-*ss*-triazine 15: Yield: 0.79 g (956.0 g/mol, 41%). 1HNMR (400 MHz, $CDCl_3$): $\delta = 10.61$ (s, 2H), 9.47 (s, 1H), 9.21 (d, 2H, 8 Hz), 9.07 (d, 1H, 8 Hz), 9.04 (d, 2H, 8 Hz), 8.54 (d, 2H, 8 Hz), 8.32 (d, 1H, 8 Hz), 8.09 (d, 2H, 8 Hz), 8.06 (d, 2H, 9 Hz), 8.02 (d, 2H, 9 Hz), 7.71–7.65 (m, 5H), 4.62 (q, 4H, 7 Hz), 4.59 (q, 4H, 7 Hz), 4.02 (s, 3H), 1.544 (t, 6H, 7 Hz), 1.51 (t, 6H, 7 Hz) ppm. 13CNMR (100 MHz, CD_2Cl_2): $\delta = 172.1$, 171.5, 168.4, 168.0, 166.9, 136.9, 134.9, 134.5, 134.1, 133.7, 132.6, 131.7, 131.5, 130.9, 130.7, 130.1, 129.9, 129.5, 129.4, 129.3, 129.1, 129.0, 128.1, 127.4, 127.2, 126.9, 126.8, 123.5, 62.8, 52.8, 14.63, 14.57 ppm. FD-HRMS: m/z calcd for $C_{59}H_{45}N_3O_{10}Na$ $[M+Na]^+$: 978.29972, found 978.3007.

Acknowledgements

We are grateful to INCT/INEO, CNPq, FAPESC, H2020-MSCA-RISE-2017 (OCTA, #778158), CAPES (Coordenação de aperfeiçoamento de pessoal de nível superior, Brazil. Finance code #937-20 and #001) and COFECUB (Comité français d'évaluation de la coopération universitaire et scientifique avec le Brésil) (joint project Ph–C 962/20) for support. The XRD experiments were carried out in the Laboratório de Difração de Raios X (LDRX/UFSC). FNdS and HML are grateful to the French ministry for Foreign Affairs for Eiffel scholarships.

Conflict of Interests

The authors declare no conflict of interest.

Data Availability Statement

The data that support the findings of this study are available from the corresponding author upon reasonable request.

Keywords: columnar liquid crystal · cyclotrimerization · mesophases · molecular glass · triazine

[1] F. Tenopala-Carmona, O. S. Lee, E. Crovini, A. M. Neferu, C. Murawski, Y. Olivier, E. Zysman-Colman, M. C. Gather, *Adv. Mater.* **2021**, *33*, 2100677.
[2] D. Yokoyama, *J. Mater. Chem.* **2011**, *21*, 19187–19202.
[3] H. Sasabe, Y. Chikayasu, S. Ohisa, H. Arai, T. Ohsawa, R. Komatsu, Y. Watanabe, D. Yokoyama, J. Kido, *Frontiers Chem.* **2020**, *8*, 00427.
[4] a) T. Woehrle, Tobias I. Wurzbach, J. Kirres, A. Kostidou, N. Kapernaum, J. Litterscheidt, J. C. Haenle, P. Staffeld, A. Baro, F. Giesselmann, S. Laschat, *Chem. Rev.* **2016**, *116*, 1139–1241.
[5] a) *Handbook of Liquid Crystals* Vol. 4, 2nd Ed. (Eds: J. W. Goodby, P. J. Collings, T. Kato, C. Tschierske, H. F. Gleeson, P. Raynes), Wiley-VCH, Weinheim, Germany, **1996**.
[6] *Chemistry of Discotic Liquid Crystals: From Monomers to Polymers* (Ed: S. Kumar), CRC Press, Boca Raton, USA, **2010**.
[7] B. Kaafarani, *Chem. Mater.* **2011**, *23*, 378–396.
[8] S. Sergeyev, W. Pisula, Y. H. Geerts, *Chem. Soc. Rev.* **2007**, *36*, 1902–1929.
[9] See Ref. [17] for a discussion of triazine-based mesogens and columnar glass formers.
[10] K. Dawson, L. Zhu, L. A. Kopff, R. J. McMahon, L. Yu, M. D. Ediger, *J. Phys. Chem. Lett.* **2011**, *2*, 2683–2687.
[11] S. E. Wolf, T. Liu, S. Govind, H. Zhao, G. Huang, A. Zhang, Y. Wu, J. Chin, K. Cheng, E. Salami-Ranjbaran, F. Gao, G. Gao, Y. Jin, Y. Pu, T. Gomes Toledo, K. Ablajan, P. J. Walsh, Z. Fakhraaia, *J. Chem. Phys.* **2021**, *155*, 224503.
[12] J. Barberá, O. A. Rakitin, M. B. Ros, T. Torroba, *Angew. Chem. Int. Ed.* **1998**, *37*, 296–299.
[13] Z. Li, M. Powers, K. Ivey, S. Adas, B. Ellman, S. D. Bunge, R. J. Twieg, *Mater. Adv.* **2022**, *3*, 534.
[14] Z. Chen, C. Bishop, E. Thoms, H. Bock, M. D. Ediger, R. Richert, L. Yu, *Chem. Mater.* **2021**, *33*, 4757–4764.
[15] A. Gujral, J. Gomez, S. Ruan, M. F. Toney, H. Bock, L. Yu, M. D. Ediger, *Chem. Mater.* **2017**, *29*, 9110–9119.
[16] C. Bishop, Z. Chen, M. F. Toney, H. Bock, L. Yu, M. D. Ediger, *J. Phys. Chem. B* **2021**, *125*, 2761–2770.
[17] F. Nunes da Silva, H. Marchi Luciano, C. H. Stadtlober, G. Farias, W. C. Costa, F. Durola, J. Eccher, I. H. Bechtold, H. Bock, H. Gallardo, A. A. Vieira, *Chem. Eur. J.* **2023**, *24*, e202203604.
[18] A. A. Vieira, G. Farias, W. C. Costa, J. Eccher, I. H. Bechtold, F. Durola, H. Bock, *Chem. Eur. J.* **2021**, *27*, 9003–9010.